A Molecular Yarn: Near-Field Optical Studies of Self-Assembled, Flexible, Fluorescent Fibers

Daniel A. Higgins, Josef Kerimo, David A. Vanden Bout, and Paul F. Barbara*

Contribution from the Department of Chemistry, University of Minnesota, 207 Pleasant Street SE, Minneapolis, Minnesota 55455

Received January 12, 1996[⊗]

Abstract: The formation of flexible molecular fibers via the solution-phase self-assembly of the pseudo-isocyanine dye (PIC) 1,1′-diethyl-2,2′-cyanine, and poly(vinyl sulfate) (PVS) is reported. The physical and electronic properties of these fibers spin-coated into thin films on fused-quartz substrates are studied by fluorescence and topographic imaging with near-field scanning optical microscopy (NSOM) and also by atomic force microscopy (AFM). The scanned-probe images demonstrate that fibers with lengths in the hundred micrometer range, widths of hundreds of nanometers, and thicknesses of a few tens of nanometers are readily formed in aqueous mixtures of PVS and PIC. Unprecedented flexibility in these fibers is exemplified by the formation of numerous curved and looped structures in the spin-coated thin films. A sandwich-like composite structure of alternating anionic PVS and cationic PIC layers is proposed as a model for the assembly of the dye and polymer in these fibers. The alternating layers in this model are held tightly together via the cooperative "cross-linking" of the PVS and PIC layers by electrostatic dye/polymer interactions, and by hydrophobic van der Waals interactions between the PIC molecules. The intermolecular interactions in the PIC layer result in the formation of a liquid-crystalline-like, well-ordered layer of the PIC which exhibits the spectral characteristics of J-aggregates. The proposed layered structure apparently possesses "reactive" surfaces which link individual fibers into a yarnlike assembly. This cross-linking effect is supported by the presence of continuous circular fibers and by the gel-forming ability of the solutions from which these fibers are grown.

Introduction

In a series of recent publications,[1−3] we have utilized near-field scanning optical microscopy (NSOM) to study the long, flexible, fluorescent fibers observed in thin films produced from aqueous mixtures of the pseudo-isocyanine dye (PIC), 1,1′-diethyl-2,2′-cyanine iodide, and the anionic polymer poly(vinyl sulfate) (PVS). NSOM is a new form of scanned-probe microscopy which utilizes light as the imaging mechanism and provides subwavelength spatial resolution in visible-light imaging and spectroscopy experiments on materials surfaces.[4−11] We utilized NSOM in our previous publications to directly study the morphological and electronic properties of the PIC/PVS fibers spin-coated onto fused-quartz substrates. In our first publication, we showed that the fluorescent nature of the fibers resulted from the self-assembly of a well-ordered, homogeneous molecular arrangement of PIC within the fibers.[1] The PIC was found to exhibit the spectral characteristics of J-aggregates,[12,13] which result from the strong coupling of the transition dipoles of individual PIC molecules, leading to the formation of new, delocalized excitonic states in the system.[14,15] In a later paper, the polarization dependence of fluorescence excitation and emission in these fibers was studied with NSOM and was employed to measure the orientation of the electronic transition dipoles of the aggregated PIC with respect to the fiber morphology.[2] These results showed that the PIC was organized in a uniform, brickstone-like structure, resulting in a herringbone-like arrangement of the monomeric PIC transition dipoles. Finally, in our third paper, picosecond time-resolved fluorescence NSOM was used to measure the lifetime of the excitonic state of the PIC aggregates in local regions.[3] These studies helped resolve issues raised in our earlier publications, such as the origin of the remarkable electronic homogeneity observed in these systems, and also the apparent limitation of excited state migration to distances of less than ∼50 nm.

In this paper, we demonstrate that the fibers formed from aqueous PIC and PVS mixtures represent novel self-assembled materials which may have important applications in thin-film optical and optoelectronic devices. We directly address the issues of fiber growth, composition, and structure with numerous optical and topographic imaging experiments utilizing the nanometer-scale spatial resolution provided by NSOM and "high amplitude noncontact" AFM. Various wet-chemical methods are also employed to aid in the elucidation of the chemical composition and structure of the fibers. The results show that the fibers are a self-assembled composite mixture of PVS and PIC. Growth of the fibers is proposed to occur through a novel noncovalent "cross-linking" of individual PVS strands

* To whom correspondence should be addressed.

[⊗] Abstract published in *Advance ACS Abstracts,* April 1, 1996.

(1) Higgins, D. A.; Barbara, P. F. *J. Phys. Chem.* **1995**, *99*, 3.
(2) Higgins, D. A.; Reid, P. J.; Barbara, P. F. *J. Phys. Chem.* **1996**, *100*, 1174.
(3) Reid, P. J.; Higgins, D. A.; Barbara, P. F. *J. Phys. Chem.* **1996**, *100*, 3892.
(4) Betzig, E.; Trautman, J. K.; Harris, T. D.; Weiner, J. S.; Kostelak, R. L. *Science* **1991**, *251*, 1468.
(5) Betzig, E.; Trautman, J. K. *Science* **1992**, *257*, 189.
(6) Dunn, R. C.; Holtom, G. R.; Mets, L.; Xie, X. S. *J. Phys. Chem.* **1994**, *98*, 3094.
(7) Ambrose, W. P.; Goodwin, P. M.; Martin, J. C.; Keller, R. A. *Science* **1994**, *265*, 364.
(8) Pohl, D. W.; Denk, W.; Lanz, M. *Appl. Phys. Lett.* **1984**, *44*, 651.
(9) Harootunian, A.; Betzig, E.; Isaacson, M.; Lewis, A. *Appl. Phys. Lett.* **1986**, *49*, 674.
(10) Rogers, J. K.; Seiferth, F.; Vaez-Iravani, M. *Appl. Phys. Lett.* **1995**, *66*, 3260.
(11) Birnbaum, D.; Kook, S.-K.; Kopelman, R. *J. Phys. Chem.* **1993**, *97*, 3091.
(12) Jelley, E. E. *Nature* **1936**, *138*, 1009.
(13) Scheibe, G. *Angew. Chem.* **1936**, *49*, 563.
(14) Czikklely, V.; Försterling, H. D.; Kuhn, H. *Chem. Phys. Lett.* **1970**, *6*, 11.
(15) Czikklely, V.; Försterling, H. D.; Kuhn, H. *Chem. Phys. Lett.* **1970**, *6*, 207.

S0002-7863(96)00105-9 CCC: $12.00

by the PIC dye. The proposed mechanism incorporates (i) electrostatic binding of cationic PIC to anionic sites along the PVS backbone and (ii) bonding of individual PIC molecules to one another by van der Waals forces. The coupling of the PIC molecules results in the formation of a well-ordered, aggregated layer of PIC along and between layers of PVS. Each PIC layer behaves as a cross-linking agent for the PVS, and in a synergistic relationship, each PVS layer effectively cross-links surrounding PIC layers together. The final product is an alternating layered structure of PIC and PVS. Such a structure is shown to have "reactive" surfaces which lead to the self-assembly of fibers hundreds of micrometers long, having widths and thicknesses in the range of tens to hundreds of nanometers.

In related work, similar polymeric materials have been studied previously because of their gel-forming abilities.[16−19] In the gel formation process, individual polymeric strands are "cross-linked" together by some mechanism to form an essentially infinite polymer network. Such gels are highly viscous materials and behave as a single entity rather than as a solution. Poly(vinyl alcohol) (PVA) is one example of such a gel-forming material which has been studied extensively.[16,17,20,21] In solutions of PVA, which is a water-soluble polymer, the OH groups along the polymer backbone can easily form hydrogen bonds to other strands of the polymer. Such a process leads, under the right conditions (temperature, ionic strength, etc.), to the cross-linking of large quantities of PVA, and ultimately to gelation. Other examples of gel formation with PVA utilize the cross-linking capabilities of ions like borate[20] and vanadate.[21] In addition, a few studies have reported the adsorption and aggregation of dyes similar to PIC along polymer strands.[16,17,22−24] However, very few publications have discussed the possibility for noncovalent cross-linking in polymeric materials such as PVA or PVS via simultaneous adsorption and self-assembly of ordered layers of organic dyes on the polymer,[16,17] and none have directly addressed such issues with high-resolution microscopic techniques like NSOM and AFM. Other highly-ordered, self-assembled systems have however been studied extensively with both far-field optical microscopy and scanned-probe microscopies.[25−28]

Experimental Section

The polymer/dye thin film samples employed here were produced from potassium poly(vinyl sulfate) (PVS) (Aldrich, average MW 140 000), which was purified as needed by reprecipitation, and 1,1′-diethyl-2,2′-cyanine iodide (PIC) (Aldrich), which was used as received. The structure of the PIC monomer, showing the ∼50° dihedral angle between the planes of the two quinoline rings[29] is depicted in Figure 1. Aqueous PVS solutions were prepared with concentrations ranging from 1 to 20 mg/mL, as specified in each experiment described below. For fiber growth, 3 mL of PVS solution was first heated to 90 °C, at which point a 0.2 mL aliquot of 10 mM PIC in methanol was added to the hot, rapidly-stirred solution. Immediately following addition of the PIC, the solution became bright orange and remained clear while hot. The presence of aggregated dye was indicated by the formation of a "gold"-colored film at the air/water interface immediately after addition of dye to the PVS solution. A small sample of the hot solution was transferred to a 200 μm thick fused-quartz substrate (Quartz Scientific) with a preheated pipet. The fused-quartz substrate, which was held at ambient temperature, was then spun at 2000 rpm on a spin-coating apparatus until dry. This procedure yielded thin films of PVS on the substrate surface incorporating a variety of morphologically-different fibrous structures, depending on the PVS solution concentration used (see below). Upon cooling to room temperature, the solutions used to produce the thin films formed cloudy, highly viscous gels at PIC concentrations at and above 330 μM. UV−vis absorption spectra of the aqueous PIC/PVS mixtures and of the spin-coated thin films indicated the presence of aggregated PIC by the appearance of the characteristic "J-band" absorption at 574 nm. The J-band dominated the absorption spectra at all PIC and PVS concentrations employed here, as shown in Figure 1.

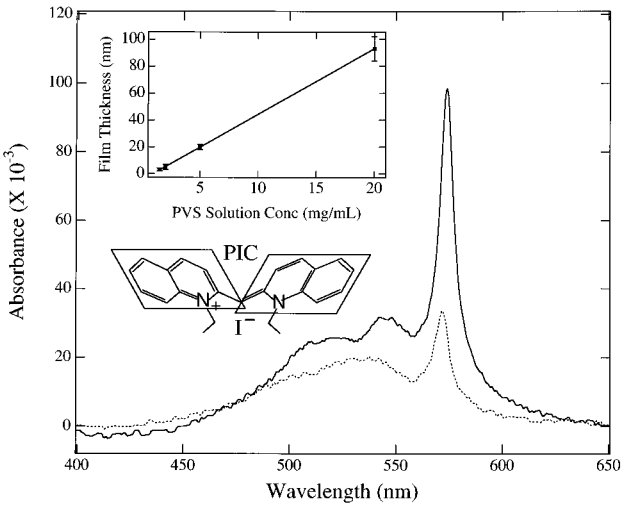

Figure 1. UV−vis absorption spectra of thin films of PIC and PVS spin-coated onto a fused-quartz coverslip. The absorption spectrum of a film prepared from a 10 mg/mL PVS and 670 μM PIC solution (—) is shown, along with the spectrum for a film deposited from a 2 mg/mL PVS and 670 μM PIC solution (- - -). The inset shows the PVS film thickness as a function of PVS concentration in the spin-coating solution. Film thickness was measured by the technique described in the text. The structure of PIC is also shown.

Film thickness in the samples studied here was determined by topographically measuring the depth of microgrooves that had been created by mechanically scraping the polymer from the substrate surface. In this procedure, an NSOM fiber probe was deliberately brought into contact with the fused-quartz surface by pushing through the polymer film. A groove of 1−2 μm width was then generated in the polymer film by scanning the sample for a short distance. The NSOM probe was destroyed by this procedure and was replaced by a new probe prior to acquisition of topographic images of the same region. A plot of groove depth was found to be linear with PVS concentration in the spin-coating solution, and is shown in the inset of Figure 1. Film thickness in central regions of the spin-coated films was found to be highly reproducible and uniform at all PVS concentrations.

A modified Topometrix Aurora NSOM was used to record all of the fluorescence near-field images and some of the topographic images presented here. This instrument has been described in detail in our previous publications.[1−3] Briefly, the Aurora employs the tapered, aluminum-coated fiber optic probes originally developed by Betzig et al.[4] as the near-field light source. Here, 0.5−1 mW of the 514.5 nm line of an argon ion laser was coupled into the probe fiber, yielding ∼10^{10} photons/s from the aperture at the end of the near-field probe (as measured in the far field). A λ/2-plate−λ/4-plate combination

(16) Shibayama, M.; Moriwaki, R.; Ikkai, F.; Nomura, S. *Polymer* **1994**, *35*, 5716.
(17) Shibayama, M.; Ikkai, F.; Nomura, S. *Macromol. Symp.* **1995**, *93*, 277.
(18) Berghmans, H.; Donkers, A.; Frenay, L.; Stoks, W.; De Schryver, F. E.; Moldenaers, P.; Mewis, J. *Polymer* **1987**, *28*, 97.
(19) Berghmans, M.; Thijs, S.; Cornette, M.; Berghmans, H.; De Schryver, F. C.; Moldenaers, P.; Mewis, J. *Macromolecules* **1994**, *27*, 7669.
(20) Kurokawa, H.; Shibayama, M.; Ishimaru, T.; Nomura, S. *Polymer* **1992**, *33*, 2182.
(21) Shibayama, M.; Adachi, M.; Ikkai, F.; Kurokawa, H.; Sakurai, S.; Nomura, S. *Macromolecules* **1993**, *26*, 623.
(22) Appel, W.; Scheibe, G. *Z. Naturforsch.* **1958**, *13b*, 359.
(23) Shirai, M.; Nagatsuka, T.; Tanaka, M. *Chem. Lett.* **1976**, *1976*, 291.
(24) Horng, M.-L.; Quitevis, E. L. *J. Phys. Chem.* **1993**, *97*, 12408.
(25) Fuhrhop, J.-H.; Helfrich, W. *Chem. Rev.* **1993**, *93*, 1565.
(26) Angelova, A.; Van der Auweraer, M.; Ionov, R.; Vollhardt, D.; De Schryver, F. C. *Langmuir* **1995**, *11*, 3167.
(27) Stabel, A.; Heinz, R.; Rabe, J. P.; Wegner, G.; De Schryver, F. C.; Corens, D.; Dehaen, W.; Süling, C. *J. Phys. Chem.* **1995**, *99*, 8690.
(28) Maskasky, J. E. *Langmuir* **1991**, *7*, 407.
(29) Dammeier, V. B.; Hoppe, W. *Acta. Crystallogr.* **1971**, *B27*, 2364.

(Special Optics) placed prior to the fiber coupler was used to control the polarization of light from the NSOM probe. The purity of polarization of the light from the tip was better than 50:1, as measured in the far field. A piezoelectrically-driven sample stage is employed in the Aurora instrument to provide sample motion in the *X*, *Y*, and *Z* (normal to the sample) directions. The sample is brought into the near field of the NSOM probe with the sample stage and is held within 5−10 nm (±1 nm) of the probe with the shear-force feedback mechanism described in detail elsewhere.[30] An oil immersion objective (100X, Zeiss Model 440280) was used to collect the fluorescence from the sample. Fluorescence from the film was isolated with two short-pass filters (CVI SWP-650) and a long-pass filter (Schott Glass OG-550). Detection of the fluorescence was accomplished with a single-photon-counting avalanche photodiode (EG&G Model SPCM-203-PQ).

A Topometrix Explorer AFM, operating in "high amplitude non-contact" mode, was also employed to topographically image the fibrous PIC/PVS thin film samples studied here. Silicon-based noncontact probes used here were obtained from Topometrix. The higher resolution, lower noise, and better-controlled forces applied to the surface by the AFM tip allow for more accurate characterization of the topographic features observed in the polymer films. However, essentially identical topographic images were produced with both the NSOM and AFM instruments. These results indicate that the shear-force feedback mechanism and the vertically-oriented NSOM probe, which may apply fairly strong forces normal to the surface, do not significantly perturb the surface of the potentially-soft films studied here.

Polarization analysis of the fluorescence from the sample was accomplished with one of two methods utilizing the NSOM instrument. The first method was described previously and involves placing an absorptive sheet polarizer (>100:1 extinction) in front of the detector.[2] Polarization-dependent images were then recorded in serial fashion with the polarizer angle fixed in one position throughout the acquisition of an image. The polarizer was then rotated to pass the orthogonal polarization, and a second image was recorded. In the second method, a broad-band (400−700 nm) polarizing beam splitter cube (Newport), with better than 1000:1 extinction of the orthogonal polarization, was employed to divide the fluorescence into two components, one polarized parallel to the scan direction and the other perpendicular. The fluorescence in the two resulting beams was detected with separate single-photon-counting avalanche photodiodes which had been previously shown to have similar responses. Two NSOM images at orthogonal polarizations were then simultaneously recorded with the Topometrix electronics, thus providing spatially-well-correlated images for accurate measurements of the degree of fluorescence polarization in the fiber samples. This new method resulted in an improvement over the first method and allowed for direct comparison of two polarization images without the problems of piezodrift and sample photobleaching, both of which are problematic in comparisons between serially-recorded images.

NSOM probes employed here were produced and characterized in-house by methods discussed extensively in the literature.[31] Fused-silica single-mode optical fiber (Thorlabs FS-SN-3224) was employed in the production of the probes. Tips with 80−120 nm diameter ends and possessing the appropriate taper[31,32] were pulled from this fiber using a CO_2-laser-based pipet puller (Sutter Model P2000). The sides of the tips were then coated with 1000 Å of 99.99% pure aluminum (Aldrich) in a vapor deposition system. A home-built apparatus was used to position the tips over the aluminum source (a tungsten boat) and to rotate them at ∼1 Hz about the fiber axis during the aluminum deposition. The pressure in the deposition chamber was maintained below $\sim 1 \times 10^{-5}$ Torr during the deposition. A shutter placed over the source was used to start and stop the deposition, which was controlled at a rate of 30−100 Å/s, as measured with a quartz crystal thickness monitor. The rate of aluminum deposition was found to be a critical factor in obtaining high-quality coatings on the tips, with faster depositions yielding smoother aluminum films. The quality of the aluminum film was characterized by viewing the tips under a conventional optical microscope with light coupled into the fiber. The smoother films showed few (if any) pinholes along the taper, as evidenced by light leakage.

Verification of the subwavelength-resolution imaging capabilities of the entire NSOM apparatus was accomplished by imaging thin-film samples incorporating single, isolated, fluorescent dye molecules. The single-molecule samples were prepared by following the procedure originally outlined by Betzig and Chichester in their publication demonstrating the use of NSOM for single-molecule detection.[33] In the preparation of these samples, fused-quartz coverslips were first coated with poly(methyl methacrylate) to yield a thin, uniform film. After this film had dried, a 20×10^{-9} M solution of 1,1′-didodecyl-3,3,3′,3′-tetramethylindocarbocyanine perchlorate (DiI, Molecular Probes No. D-383) in methanol was spin-coated on top of the polymer film. These samples were then imaged in the NSOM apparatus by excitation at 514.5 nm through the NSOM probe while monitoring the fluorescence from the film. A 530 nm long-pass filter and a 514.5 nm holographic notch filter (Kaiser Optical) were used to remove the excitation light. A near-field fluorescence image of one of these samples is shown in Figure 2a. Topographically, the film appears uniform with an average roughness of 1 nm over a 5 μm area. However, small fluorescent features are observed in the near-field image. Maximum signal levels observed for these fluorescent features are ∼300 photons/pixel with a 20 ms pixel time and ∼10 nW of 514.5 nm light from the NSOM tip. These values correspond well with those observed in previous near-field experiments on single-molecule samples.[33] The spatial dimensions of the fluorescent regions average 120 ± 20 nm full width at half-maximum. Since single molecules are much smaller in size than our NSOM probes, (∼1 nm^2 vs ∼10 000 nm^2), the fluorescent regions are essentially images of the electric field distribution in the near field of the NSOM probe. Such images can therefore be used as a direct measure of the resolution provided by a given probe. In this particular case, the results indicate that the probe diameter (and hence the spatial resolution) is ∼120 nm.

Results and Discussion

A. Film and Fiber Morphology. The morphological properties of the composite thin films of PIC and PVS were characterized here by topographic and optical microscopic methods utilizing NSOM and noncontact AFM. Parts b−d of Figure 2 show the topographic and fluorescence NSOM images of a PIC/PVS thin film deposited by spin-coating a hot (90 °C) aqueous 10 mg/mL PVS and 670 μM PIC solution onto a fused-quartz coverslip. As we have shown in our previous publications,[1−3] and as is shown again in Figure 2, fluorescent fibrous features are readily found in these films. The fibers in Figure 2 yield a maximum fluorescence count rate of 9000 photons/s (excited with $\sim 10^{10}$ photons/s) and are dispersed in a nonfluorescent (200 counts/s) film of PVS. Under these particular film preparation conditions, the fluorescent fibers are extremely long and essentially "one-dimensional" with macroscopic lengths of hundreds of micrometers and average widths 1000 times smaller (130 ± 20 nm, from Figure 2).

The actual lengths of these fibers are difficult to determine because fiber ends are rarely observed in NSOM images, due to the limited scan range. However, the entire lengths of the largest fibers are sometimes visible under a conventional, far-field microscope, albeit at much lower spatial resolution. Topographic images of the fibers have also been obtained with the Explorer AFM, for which a larger scan range is available. The larger scan range allows for location and imaging of fiber ends. An example of these images is shown in Figure 3a. Indicative of the length of the fibers is the fact that very few ends are observed in Figure 3a, despite the 50 μm scan range. Somewhat better spatial resolution is also available with the

(30) Betzig, E.; Finn, P. L.; Weiner, J. S. *Appl. Phys. Lett.* **1992**, *60*, 2484.

(31) Valaskovic, G. A.; Holton, M.; Morrison, G. H. *Appl. Opt.* **1995**, *34*, 1215.

(32) Yakobson, B. I.; Moyer, P. J.; Paesler, M. A. *J. Appl. Phys.* **1993**, *73*, 7984.

(33) Betzig, E.; Chichester, R. J. *Science* **1993**, *262*, 1422.

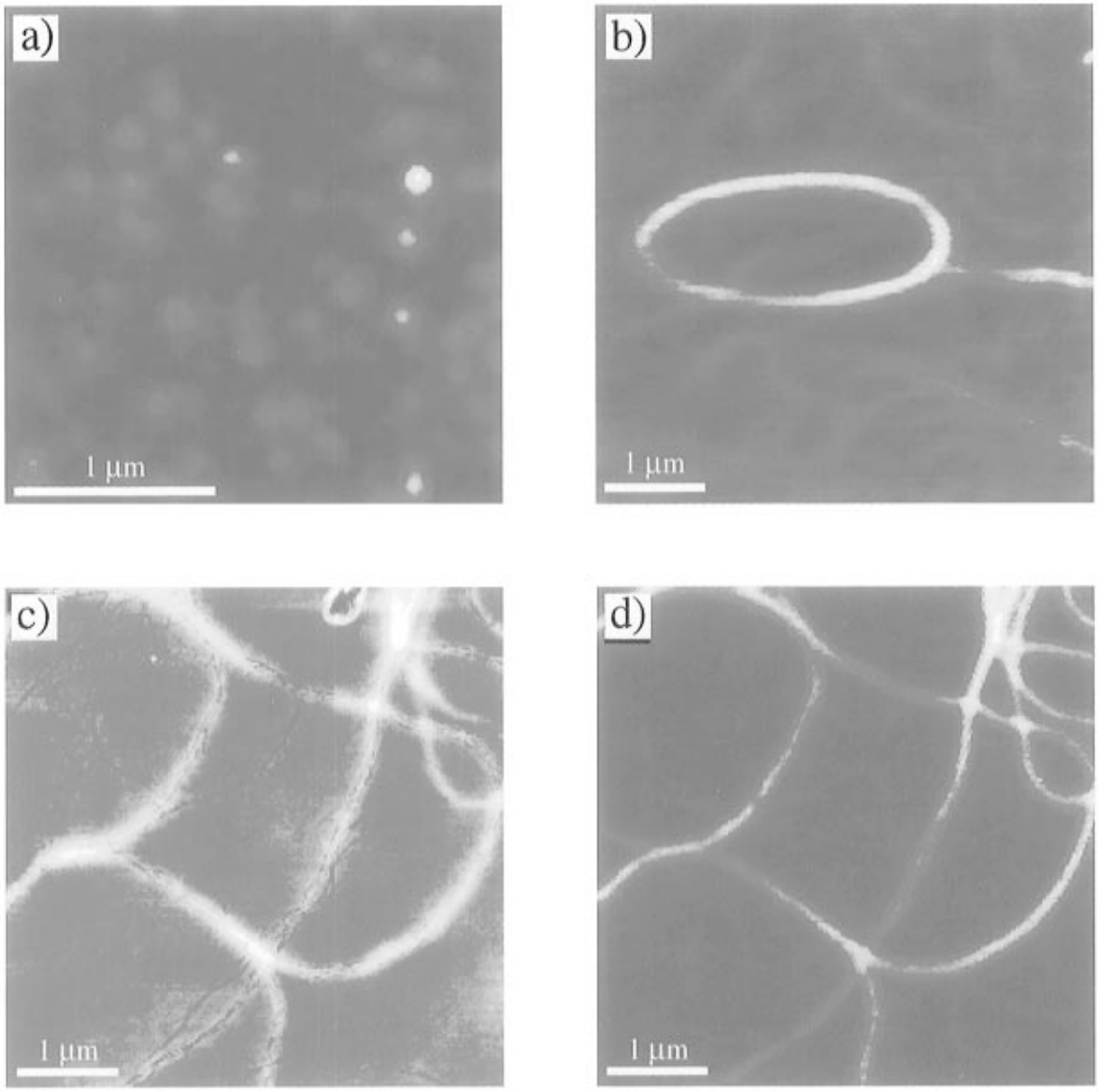

Figure 2. (a) Fluorescence near-field image of a sample prepared by spin-coating a 20 nM methanolic solution of DiI onto a thin film of poly(methyl methacrylate) which is supported on a fused-quartz coverslip. The fluorescent regions of the film result from excitation and detection of the fluorescence from single, isolated DiI molecules. (b) A fluorescence NSOM image of a thin PVS film incorporating fluorescent fibers. The film was produced by spin-coating a 10 mg/mL PVS and 670 μM PIC solution onto a fused-quartz substrate. Important evidence for the flexibility of the observed fibers is given by the observation of highly curved fibers, such as the continuous loop shown here. (c) A topographic image of a similar sample acquired with the NSOM instrument. The fibers are seen partially buried in the otherwise uniform PVS film of 45 nm thickness. An average height of 5 nm is measured for the fiber topography in this image. (d) The fluorescence NSOM image collected simultaneously with the topographic image in (c).

AFM (routinely <10 nm) in comparison to topographic images recorded with the NSOM. Images recorded with the AFM have revealed that the fibers described here are actually comprised of a bundle of much smaller fibers. The presence of the smaller fibers is evidenced in images of fiber ends, as shown in Figure 3b−d. The smaller fibers appear in these images as what look like the "frayed" ends of a larger, single fiber. These results show that the large fibers observed here, which have average widths of 160 ± 60 nm, are assembled from smaller fibers with average widths of 30 ± 5 nm. Similar effects have been observed previously by scanning electron microscopy for other types of aggregates.[34]

While lengths and widths for these fibers are measurable with NSOM and AFM, their thicknesses are much more difficult to obtain by such means. The difficulty in measuring their thicknesses results from the fact that most fibers are at least partially buried in the polymer film, as shown in Figure 2c,d. The buried fibers in these films are easily observed in fluorescence NSOM images, but are sometimes absent from the topographic images, from which thicknesses are most readily determined. However, an upper limit for the thicknesses of these fibers can be estimated from the thickness of the PVS film itself. For films prepared from 10 mg/mL PVS solution, the average film thickness has been determined to be 45 ± 4 nm by the technique described above. Fibers which show no topography can therefore be no thicker than 45 nm in these particular samples.

In some cases, fibers have been found to lie completely exposed on top of the polymer film, thus allowing for direct measurement of their thicknesses. Verification that a particular fiber lies entirely above the polymer surface is obtained from noncontact AFM images of regions where multiple fibers cross,

(34) Emerson, E. S.; Conlin, M. A.; Rosenoff, A. E.; Norland, K. S.; Rodriguez, H.; Chin, D.; Bird, G. R. *J. Phys. Chem.* **1967**, *71*, 2396.

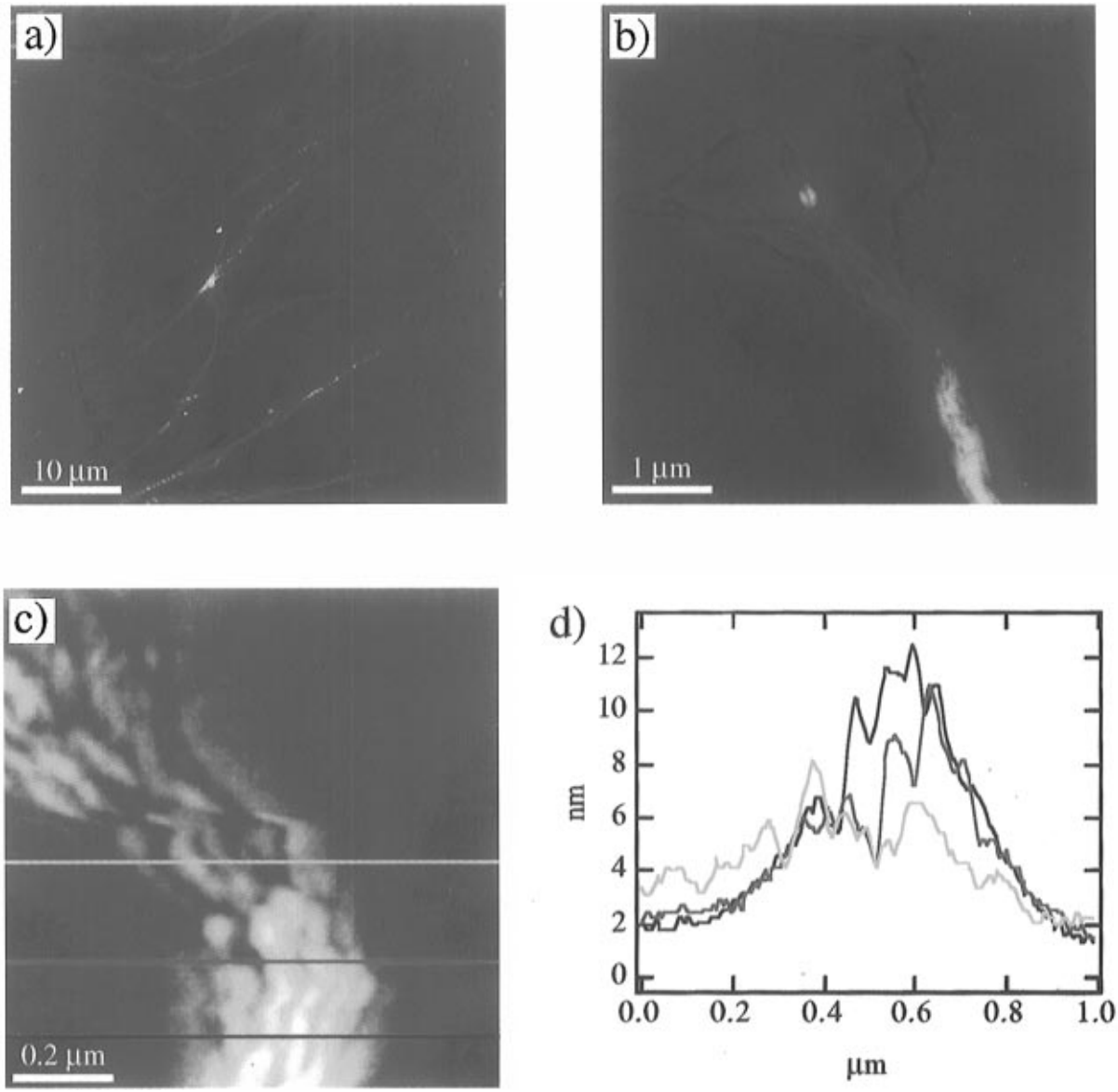

Figure 3. (a) A noncontact AFM image of a thin film of PVS and PIC incorporating the fluorescent fibers. This image shows that the fibers are extremely long, with only a few fiber ends visible in the image. In addition, the appearance of fibers with curves as small as 500 nm in radius proves that the fibers are extremely flexible. (b) A noncontact AFM image of a fiber end showing that the main portion of the large fiber is ~160 nm wide and is assembled from many smaller fibers of ~30 nm widths. (c) A smaller region imaged at the very end of the fiber shown in (b) showing the presence of the much smaller fibers. (d) Topographic line scans from (c).

as shown in Figure 4. In such images, the topography at the crossing point has frequently been observed to equal the sum of the heights of the individual fibers on either side of the intersection. The linear relationship between the individual fiber heights and the height at the intersection indicates that the fibers are on top of the polymer film. Had the fibers been significantly submerged in the polymer, the height at the cross would be expected to be different from the sum of their individual heights. Measurements of fiber thicknesses by this method indicate that they are nominally 10 nm thick for films grown from these particular PIC/PVS solutions.

While the issue of fiber composition and structure will be discussed in the following section, the observed morphology of the PVS film in the proximity of the fibrous features suggests a difference in physical properties (i.e., density, extent of solvent swelling) between the fibers and the surrounding PVS film. As is shown in Figure 2c, fibers buried in the polymer film are sometimes accompanied by the appearance of a slight "crack" or depression in the topographic image of the film surface. The high spatial resolution in this particular topographic image comes from the presence of a sharp feature on the end of the NSOM probe. The depressions observed in Figure 2c, as well as in many other images, may be due to shrinking of the PVS film around the fibers. The PVS film is most certainly swelled to a significant extent in its hydrated state and would be expected to shrink upon drying during the spin-coating process. The appearance of the cracks in the vicinity of the fiber therefore suggests that the fibers do not undergo significant swelling and may possibly be formed with a much more densely-packed molecular structure.

One of the most noteworthy physical attributes of the fibers is their apparent flexibility, as evidenced by the appearance of highly curved fibers in Figures 2 and 3 and in virtually every other image of these films.[1,2] In some images, continuous loops in individual fibers are even observed, as in Figure 2b. These bends and loops form on microscopic distance scales with some curve radii as small as 500 nm. The curved features in these fibers are most likely created during the deposition process in which fibers formed in the PVS/PIC solution are dropped onto the substrate surface prior to spin-coating. Mechanical defor-

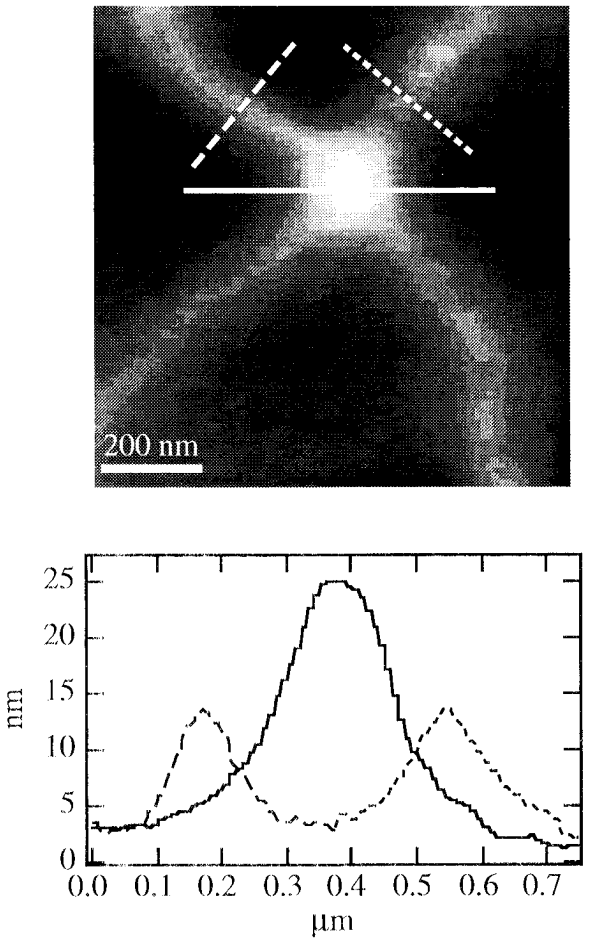

Figure 4. An AFM image and line scans of the intersection between two fibers. The image shows that these particular fibers are completely exposed on top of the PVS film as evidenced by the additivity of the individual fiber heights in the line scans.

mation of the fibers during deposition produces the curved structures. Such a mechanism requires that the fibers be highly flexible and presupposes that they form mostly in solution prior to deposition. Evidence for the formation of the fibers in the solution phase, rather than growth within the film itself, is supported by the observed concentration of the dye in the fibrous structures, resulting in the formation of a highly heterogeneous film. The dye would not be expected to diffuse through the polymer film to form such concentrated fibers during the spin-coating and film-drying processes.

B. Fiber Composition and Structure. As noted above, the fibers observed in these films are highly fluorescent in comparison to the background of the surrounding polymer film (9000 counts/s maximum vs 200 counts/s in Figure 2). The vast majority of the PIC dye must therefore be concentrated in the fibers. The spectral characteristics of the fluorescence was determined by recording local fluorescence spectra with the NSOM apparatus. Such measurements were made with 100 nm spatial resolution by positioning the near-field probe over a particular region of a single fiber and sending the fluorescence from that fiber to a monochromator and liquid-N_2-cooled CCD. The spectra unequivocally show that the PIC incorporated in the fibers is present in an aggregated state. These fluorescence spectra are dominated by a narrow, red-shifted (from that of monomeric PIC) fluorescence peak positioned at 574 nm.[1] No fluorescence from residual monomeric dye species is observed in these fibers, although it is probable that some exists at very low concentration in the nonfibrous regions of the PVS film. In addition to the fluorescence results, bulk UV−vis absorption spectra acquired for these films show similar changes from the monomeric dye spectra (see below). The new spectral features are characteristic of the formation of excitonic states in a tightly-packed, highly-ordered brickstone-like arrangement of dye molecules.[1,2,14,15] Systems such as these are traditionally known as J-aggregates.[12,13] From the above results, it can therefore be concluded that these fibers are constructed in part from a well-ordered array of PIC molecules.

Polarization-dependent imaging with NSOM provides further information on the organization of the PIC molecules within the fibers. In these experiments, the polarization dependence of both excitation to and emission from the excitonic states formed in these fibers is recorded and is used to determine the transition dipole orientations. The orientation of the transition dipole for the lowest energy electronic transition in this system (known as the J-band) can be directly measured by polarization analysis of the fluorescence from the fibers, as we have demonstrated in a previous publication.[2] Here, two images of the ring shown in Figure 2b were recorded and are shown in Figure 5. The image in Figure 5a was recorded with the analyzer oriented perpendicular to the scan direction (vertical on the page). The analyzer was oriented parallel to the scan direction in Figure 5b. From these results, it is obvious that the fluorescence is polarized parallel to the long axis of the fibers, indicating that the transition dipole to the lowest energy excitonic state in the fibers is oriented parallel to the fiber axis. Extinction ratios for cross-polarized fluorescence detection in the images in Figure 5 are as high as 10:1. In our previous publication, we showed that fluorescence excitation in this same spectral region (at 570 nm) was also dramatically more efficient for light polarized along the long axis of the fibers.[2]

The above results are entirely consistent with the traditional model for J-aggregates in which the transition dipoles of the individual monomers are aligned parallel to one another in a brickstone-like arrangement.[14,15] Such an arrangement would yield one allowed transition to the excitonic band.[35] However, as has been noted in numerous other works,[36−38] and as is evidenced in Figure 6, there is a higher energy transition which is also allowed in this system. Figure 6 shows that the absorption spectrum of the J-aggregates includes bands at 537 and 502 nm in addition to the J-band at 572 nm. The higher energy bands are distinct from those of the monomer at 523 and 490 nm and are certainly part of the excitonic spectrum.[37,38]

The polarization dependence of fluorescence excitation in the higher energy region of the spectrum is not as pronounced as in the J-band region, however, as has been shown previously.[2,36,38] It is found here that excitation by light polarized perpendicular to the long axis of the fibers is slightly more efficient than for parallel polarization. In our previous studies we found that excitation at 514.5 and 488 nm showed 1.1:1 and 1.3:1 preferences for short- vs long-axis polarized excitation.[2] Interference from vibronic transitions to the lowest energy excitonic state (long-axis-polarized) reduces the polarization ratios observed here.[37] However, it can be concluded from these results that the higher energy transition dipole must be oriented perpendicular to the long fiber axis.

When all of the polarization-dependent data are taken in concert, along with the noted presence of an allowed transition to a higher energy excitonic state, it can be concluded that the monomeric transition dipoles coupling to form the excitonic

(35) McRae, E. G.; Kasha, M. *J. Chem. Phys.* **1958**, *28*, 721.
(36) Scheibe, G. *Lage, Intensität und Struktur von Absorptionbanden*; Scheibe, G., Ed.; Verlag Chemie: Wienheim, 1966; p 109.
(37) Scherer, P. O. J.; Fischer, S. F. *Chem. Phys.* **1984**, *86*, 269.
(38) Misawa, K.; Ono, H.; Minishima, K.; Kobayashi, T. *Appl. Phys. Lett.* **1993**, *63*, 577.

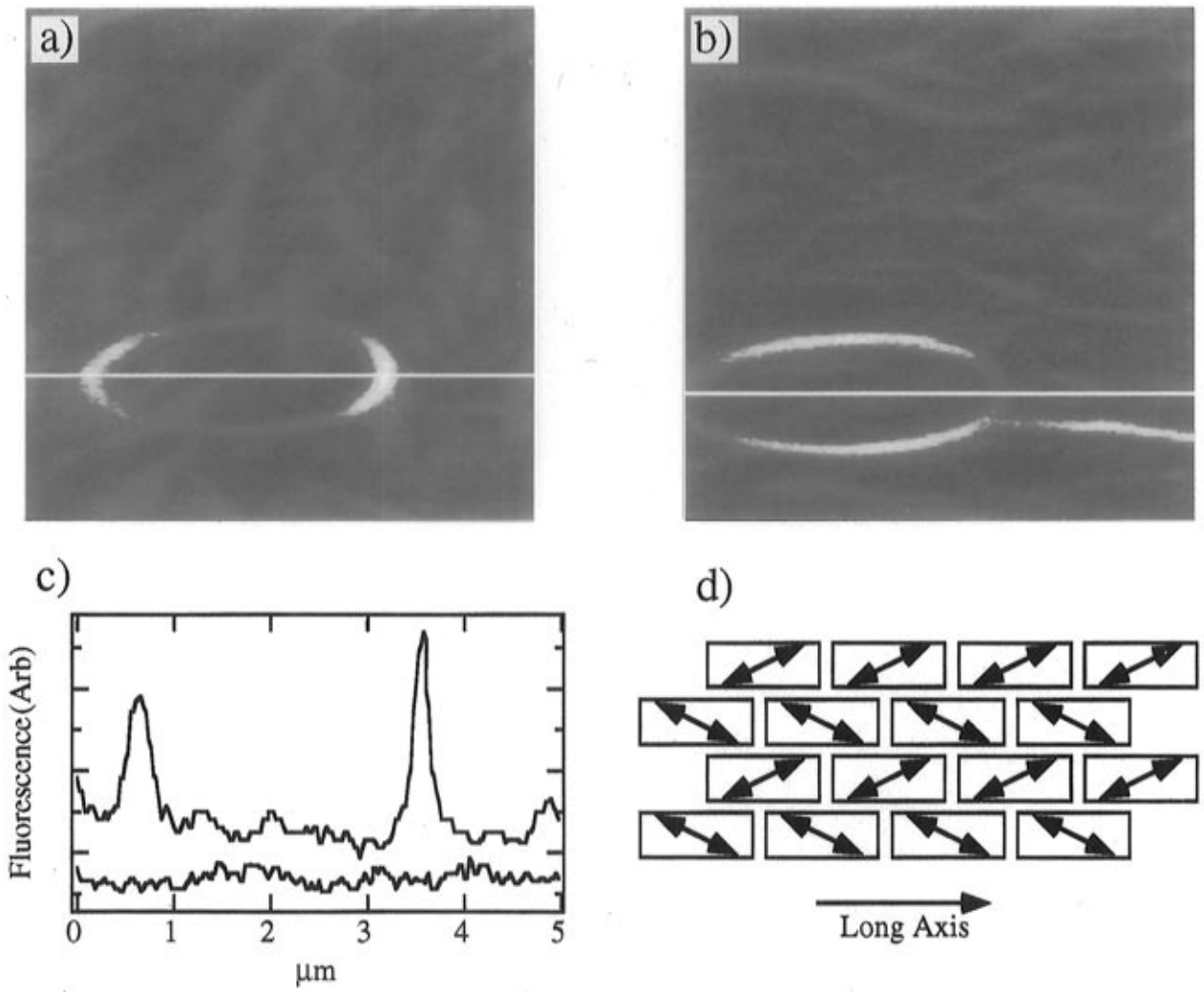

Figure 5. Polarization-dependent fluorescence near-field images of a ringlike fiber. Images were recorded by detection of (a) fluorescence polarized vertically on the page (perpendicular to the scan direction) and (b) fluorescence polarized horizontally on the page (parallel to the scan direction). These images prove that the fluorescence from these fibers is well-polarized along the long axis of the fibers. (c) Line scans across these images are presented, showing a 10:1 extinction ratio for orthogonal polarizations. The baselines of the two line scans are offset for clarity. (d) A model for the herringbone-like arrangement of monomeric transition dipoles in the PIC J-aggregates present in these fibers. The space filled by an individual molecule is represented by the rectangular "bricks" in the model; the arrows represent the transition dipole directions.

band of the aggregate are likely organized in a herringbone-like geometry, as is diagrammed in Figure 5d.[2,35,39] Such a system is known to yield two allowed transitions to the excitonic band,[39] as is observed here. It has been shown in previous publications that, for PIC aggregates, this herringbone arrangement of transition dipoles in a brickstone-like arrangement of PIC molecules is a result of the nonplanarity of the PIC dye monomer (see Figure 1).[29,40] The nonplanarity of the dye leads to the tilting of individual transition dipoles off the long axis of the aggregate fibers. A similar arrangement of monomers has been determined for other aggregated systems by electron diffraction methods.[41] The results presented above prove that highly-organized J-aggregates of PIC are a major component of the fluorescent fibers observed in the NSOM images.

The tremendous flexibility of the fibers, the gel-forming propensity of the spin-coating solutions used in their production, and the results of numerous wet-chemical experiments suggest that PVS is also an integral component of the fibers. In the wet-chemical experiments, the ability of a series of solutions of different ionic species to form fibers in the presence of PIC was evaluated and compared to that of PVS solutions. The fiber-forming ability was evaluated by noting whether aggregates were produced in a given solution, as measured via changes in the UV−vis absorption spectrum of the bulk solution. A number of different aqueous inorganic− and polymer− electrolyte solutions were investigated. In all cases, PVS solutions were found to form PIC aggregates at the lowest dye concentrations and at the lowest ionic strengths. Preparations in which PVS was replaced by 0.03 M Na_2SO_4 (approximately the same ionic concentration as 10 mg/mL PVS) lead to no J-aggregate formation at 330 μM PIC, as shown in the data presented in Figure 6. In contrast, strong J-aggregate formation was observed in PVS solutions with more than 10 times lower ionic concentration (see Figure 1). J-aggregates were also found to form in 0.06 M KCl solutions, but not to the same extent. In these solutions, the monomer bands at 523 and 490 nm dominate the spectrum (see Figure 6). Finally, when PVS was replaced by poly(styrenesulfonate), no aggregates were observed to form at all, as evidenced by the observation of unperturbed PIC monomer in the spectrum shown in Figure 6.

The greatly enhanced aggregation of ionic dyes similar to PIC in solutions of ionic polymers of opposite charge has been reported numerous times in the literature.[16,17,23,24] These

(39) Hochstrasser, R. M.; Kasha, M. *Photochem. Photobiol.* **1964**, *3*, 317.
(40) Nolte, H. J. *Chem. Phys. Lett.* **1975**, *31*, 134.
(41) Duschl, C.; Frey, W.; Knoll, W. *Thin Solid Films* **1988**, *160*, 251.

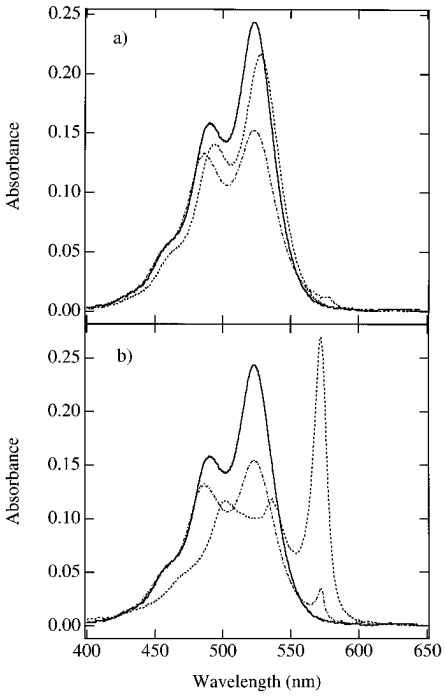

Figure 6. UV−vis absorption spectra for bulk solutions of PIC and various inorganic and polymer electrolytes. (a) Spectra for monomeric PIC in methanol (—), PIC in poly(styrenesulfonate) (- - -), and PIC in Na_2SO_4 (- · -) are shown. (b) Spectra for aggregated PIC (- - -) in PVS and PIC in KCl (- · -) are shown along with monomeric PIC (—) for comparison. Ionic strengths of all electrolyte solutions are ~0.06 M. The results show that aggregation is significantly enhanced in PVS over all other solutions studied here, indicating that there are very specific electrostatic and steric effects that make J-aggregate formation with PVS more favorable. It can therefore be concluded that the PVS is an integral component of the fibers.

previous works point to the importance of electrostatic adsorption of the ionic dye to the polymer. However, as is evidenced by the lack of PIC aggregation on poly(styrenesulfonate), aggregation of the dyes on the polymer is a complex process and must also be highly dependent on structural properties, such as the match between ionic group spacing on the polymer and the required spacing for aggregation of the dye. Since PIC J-aggregates are readily formed in PVS solutions and are not formed at all in poly(styrenesulfonate) solutions of the same ionic concentration, it can be concluded that PVS is definitely incorporated in the fibers observed here and plays an important role in the aggregation of PIC in this system.

A model for the possible structure of the fibers, incorporating both PIC and PVS, is proposed here and is diagrammed in Figure 7. In this model, it is proposed that the PIC molecules and PVS polymer self-assemble into a layered structure from the monomeric dye and single strands of polymer. The dye molecules are tightly bound to the polymer through the electrostatic attraction of the cationic dye to the anionic sites on the PVS. The polymer-bound dye molecules then self-assemble into the well-ordered arrangement presented above and are held together via van der Waals forces. In such a model, the alternating layers are held together by a novel, noncovalent cross-linking mechanism in which the PIC links surrounding layers of PVS together and the PVS strands act to link the alternate layers of PIC together. Note that, as shown in Figure 7, and as has been proposed previously,[40] the PIC molecules in such a structure are organized in an alternating up−down fashion. While the NSOM measurements presented here can only provide direct information on the organization of the fluorescent PIC molecules and not on the incorporated PVS,

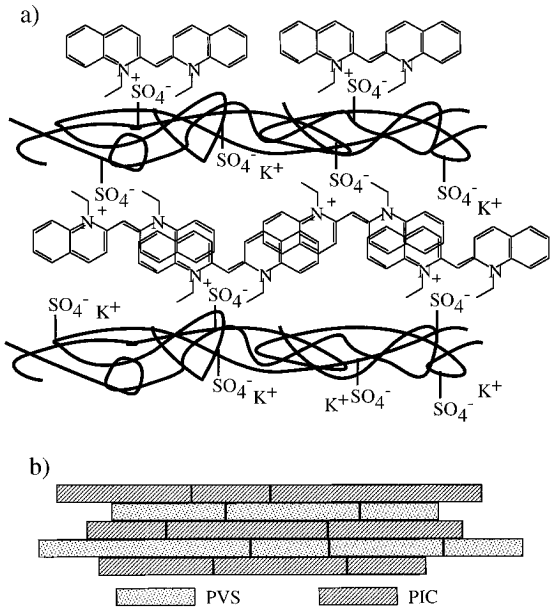

Figure 7. Structural model (a) on the molecular scale and (b) on the fiber dimensional scale proposed for the PIC/PVS composite fibers. For simplicity, the PIC molecules are drawn as being planar in (a). The structure is held together by a novel noncovalent cross-linking mechanism. In this structure, dye is bound to the PVS by electrostatic forces and polymer-bound dye molecules are held together and are organized into the aggregated structure shown in Figure 5d by van der Waals forces.

it is proposed that the polymer layer is somewhat disordered, with anionic groups protruding in many directions and allowing for the linking of various layers of PIC aggregates together. It should be noted that this model represents only one of a number of possibilities for the formation of the fibers observed here.

C. Fiber Growth Mechanism and Pseudochemical Fiber Interactions. The model for the fiber structure presented above suggests a mechanism for growth of the fibers. As shown in Figure 7, the surfaces and ends of the fibers, which may be comprised of a single strand of PVS with dye complexed to it, are expected to be reactive toward coupling to other fibers, or toward adsorption of uncomplexed dye or polymer. Such effects have already been noted in the AFM images presented in Figure 3b−d. In those images, the ends of larger fibers are shown to "break-up" into smaller fibers. This behavior suggests that the larger fibers are comprised of smaller fibers that have clustered together.

A similar conclusion is also suggested by the dependence of fiber morphology on the PVS concentration used in the spin-coating solution. As the concentration of PVS in the aqueous solution is reduced, the fibers observed in the NSOM and topographic images become smaller. Parts a and b of Figure 8 depict the shear-force topography and fluorescence NSOM images of a film sample grown from 5 mg/mL PVS solution, again with 670 μM PIC. Fluorescent fibers showing the spectral characteristics of PIC J-aggregates are once again observed in the near-field images. However, the fibers now appear much narrower than those discussed above, with average widths of 100 ± 10 nm. The measured fiber widths in these samples are now most likely limited by the spatial resolution of the NSOM tips employed here. Their thicknesses are assumed to be in the monolayer to few monolayer range since they are rarely observable above the noise (± 1 nm) in the topographic images. Most noticeable, however, is the dramatic change in the microscopic order in the film. The fibers produced from this solution appear to be much more well-aligned with respect to neighboring fibers than at the higher PVS concentrations. Such

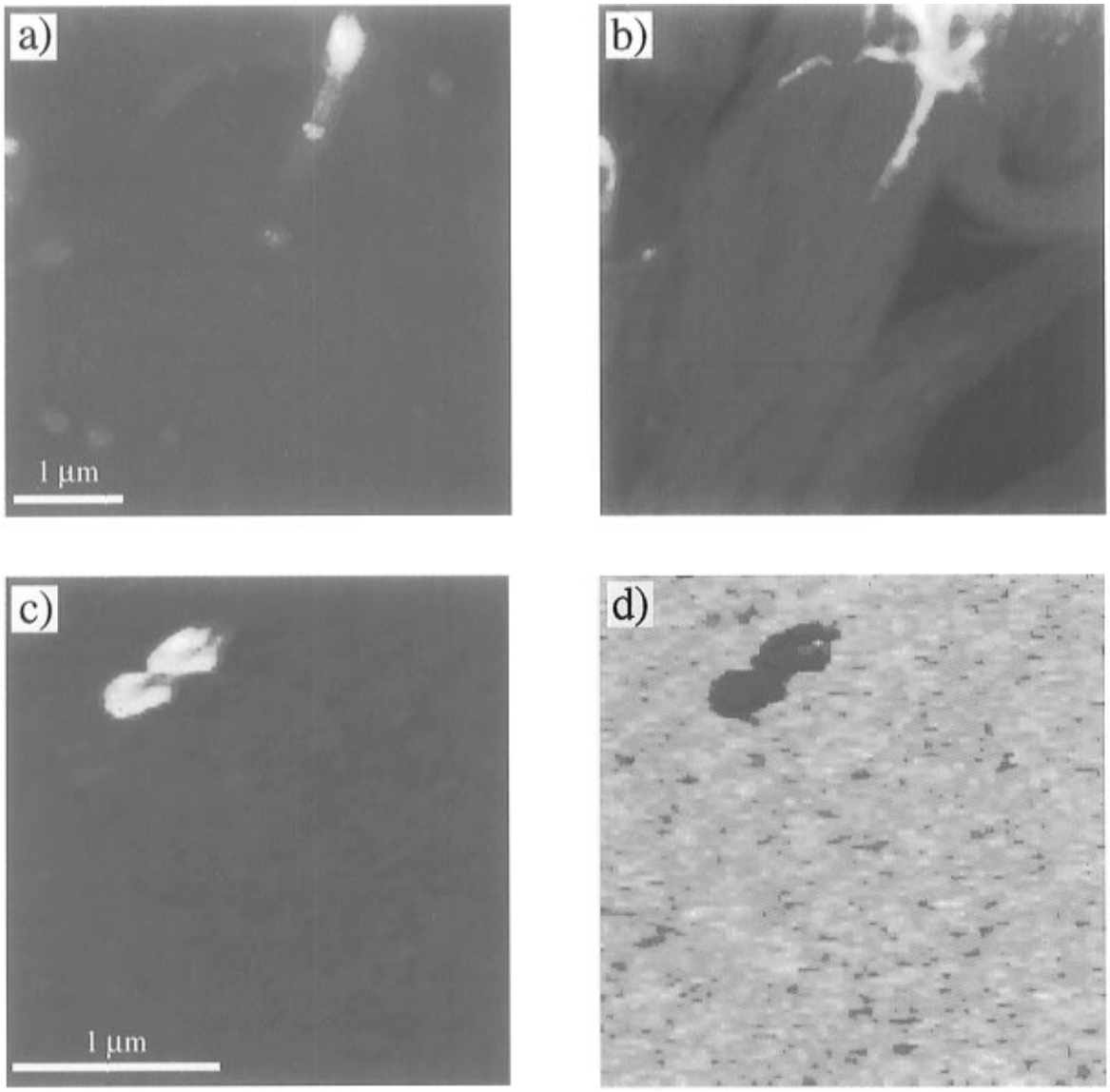

Figure 8. Topographic (a) and fluorescence NSOM (b) images of PVS/PIC fibers grown from 5 mg/ML PVS and 670 μM PIC solution. Topographic (c) and fluorescence NSOM d) images of PVS/PIC fibers grown from 1 mg/ML PVS and 670 μM PIC solution. The two features which appear dark in the fluorescence image in (d) are either nonfluorescent impurities on the film or particles of non-dye-doped PVS. The images show that the larger fibers observed at the higher PVS concentrations are likely formed from the linking together of smaller fibers, as shown in Figure 3b−d.

an effect likely results from the reduction in the viscosity of the spin-coating solution as the PVS concentration is reduced. The spin-coating process then mechanically aligns the fibers in this sample.

As the PVS concentration is reduced further, fibers are no longer easily observed in either the topographic or fluorescence NSOM images. A fluorescence NSOM image recorded for a film deposited from 1 mg/mL PVS solution (with 670 μM PIC) is shown in Figure 8c,d. The film appears uniformly fluorescent here; however, it is likely that fibers are present in this film but are simply too small to be observed with the present spatial resolution. The highest resolution obtainable with current NSOM technology[4] cannot be reached here due to the low fluorescence quantum yield for these samples ($\sim$0.006)[3] which requires high excitation intensities and, therefore, large tips to yield measurable fluorescence signals. The film does however show the same spectral features of PIC J-aggregates (see Figure 1) as at the higher PVS concentrations.

While the growth of these fibers most likely occurs via a complicated mechanism that involves both kinetic and thermodynamic limitations, the reactive nature of the fiber surfaces is indicated by the appearance of continuous fiber rings which are occasionally observed in the PIC/PVS films. One such fiber is shown in Figure 2b and also in Figure 5. Note that no apparent breaks are observed in these images where the two ends of a single fiber might have grown together. Such a seam may be too small to observe with the spatial resolution of the NSOM instrument, but may also indicate that the two ends were actually bonded together early in the growth process. Continued adsorption of other fibers, polymer, or dye then further coupled the ends and covered the original seam.

The final piece of evidence for the fiber growth mechanism proposed here comes from the physical properties of the PIC/PVS solutions employed in film production. As noted above, upon cooling, the solutions of highest dye and polymer concentrations were found to form very viscous, cloudy gels. Gels are known to form from highly cross-linked polymeric materials.[16−21] The gel-forming ability of the PIC/PVS solutions therefore suggests that the fibers present in this system are readily coupled into a highly cross-linked network. The reactive surfaces provided by uncomplexed dye and uncomplexed polymer on the surface of the model fiber proposed in Figure 7 provide a likely means for this cross-linking to occur.

Conclusions

In summary, long, flexible, fluorescent fibers have been produced by self-assembly of well-ordered PIC J-aggregates and PVS. The fibers were investigated by fluorescence NSOM and by noncontact AFM. These results show that the largest fibers have lengths of hundreds of micrometers, widths of a few hundred nanometers, and thicknesses of a few tens of nanometers at most. The fibers are proposed to form via the coupling together of much smaller fibers, possibly comprised of single strands of PVS with adsorbed PIC. Furthermore, these fibers are proposed to assemble into larger fibers by a novel noncovalent cross-linking mechanism which involves the synergistic coupling of cationic dye to anionic polymer followed by coupling of individual polymer-bound dye molecules together via van der Waals forces. The coupling of the polymer-bound dye molecules results in the formation of a highly-ordered layer of the dye in the fibers which exhibits the spectral characteristics of J-aggregates. The surfaces of the fibers are thought to be highly reactive with many uncomplexed anionic sites on the polymer and uncomplexed cationic sites in the aggregate layer near the surface. The surface "reactivity" of these fibers is directly evidenced by the formation of continuous fiber loops, which appear to show no "seams", and by the observed gel-forming abilities of solutions of these fibers. While long fibers are produced during aggregation of the dye alone, the incorporation of the polymer in the fibers renders them much more flexible, as evidenced by the prevalence of curves and loops in the fibers imaged here.

Acknowledgment. The authors acknowledge the support of the Office of Naval Research and the University of Minnesota in these studies. D.A.H. and D.A.V.B. gratefully acknowledge the National Science Foundation Postdoctoral Fellowship Program for their support.

JA960105V